Research Article

Husam Abdulrasool Hasan*, Jenan S. Sherza, Azher M. Abed, Hakim S. Sultan and Kamaruzzaman Sopian

Improve the performance of solar thermal collectors by varying the concentration and nanoparticles diameter of silicon dioxide

https://doi.org/10.1515/eng-2022-0339
received April 25, 2022; accepted June 07, 2022

Abstract: The influence of different concentrations and nanoparticles' diameter of silicon dioxide nanoparticles on the Nusselt number enhancement ratio and friction factor for solar thermal collector (STC) was examined numerically. The CFD model was designed to show the influence of the flow of water/SiO_2 and pure water inside the pipe on the enhancement of the performance of the STC. Different concentrations of SiO_2 nanoparticles are used (ϕ = 1–4%) with several nanoparticle diameters (dp = 20–50 nm). The water/SiO_2 and pure water flow under different Reynolds numbers ranging from 5,000 to 30,000. The average Nusselt numbers Nu_{avg} improved by increasing the Reynolds numbers for both fluids. The Nu_{avg} increases with the increase in the concentration of SiO_2 nanoparticles. The water/SiO_2 with nanoparticle concentration of (ϕ = 5%) and nanoparticle diameter of (dp = 20 nm) has the highest Nusselt number. The Nu_{avg} enhances 25% with water/SiO_2 nanofluid flow at Re = 5,000 and 15% flow at Re = 30,000. It is noted that the skin friction factor decreases with the increase in the Reynolds number for both fluids. Water/SiO_2 nanofluid has a higher skin friction factor than pure water. The Nu_{avg} improved by 31% at the lowest Reynolds number by using water/SiO_2 nanofluid as the working fluid with a change in the concentration of SiO_2 nanoparticles from (ϕ = 1%) to (ϕ = 4%) and improved by 42% at the highest Reynolds number of 30,000. The decrease in the nanoparticle diameter led to an increase in the Nusselt number across all Reynolds numbers. The lowest size SiO_2 nanoparticles (dp = 20 nm) provides the highest Nusselt number. The lowest size SiO_2 nanoparticles (dp = 20 nm) provide the highest ratio of enhancement for the Nusselt number in STC. This investigation has confirmed that the flow of water/SiO_2 with AL_2O_3 nanoparticles of 5% (diameter of 20 nm) has a significant influence on heat transfer enhancement to improve the thermal efficiency of STC.

Keywords: nanofluids, solar thermal collector, silicon dioxide nanoparticles, heat transfer

1 Introduction

The increasing population has resulted in increased electricity consumption in development projects. Home energy usage includes water heating, space heating, and air conditioning. Environmental and security aspects separate solar from other energy sources. Solar energy was employed to heat water in the last decades. Using nanofluid as a functional fluid may improve solar heat absorption. Using nanofluids as circulating liquids is one technique to enhance solar thermal performance. Traditional thermal transfer fluids were mixed with nano-sized metallic particles for nanofluid. A nanofluid consists of nanometer-sized metals, oxides, carbides, or carbon particles in a base fluid [1]. The effect of combining corrugated barriers and nanofluids on solar heater collector performance was explored. Different nanoparticle concentrations were investigated [2]. Carbon nanoplatelets and metal oxide nanoparticles were employed to create water-based nanofluids. The researchers discovered that using nanofluids increased

* **Corresponding author: Husam Abdulrasool Hasan,** Department of Air Conditioning & Refrigeration Techniques, Al-Esraa University College, Baghdad, Iraq, e-mail: drhusam@esraa.edu.iq, hussam2003hussam@yahoo.com
Jenan S. Sherza: Department of Air Conditioning & Refrigeration Techniques, Al-Esraa University College, Baghdad, Iraq
Azher M. Abed: Department of Air conditioning and Refrigeration, AL-Mustaqbal University College, Babylon, Iraq, e-mail: dr.azhermuhson@gmail.com
Hakim S. Sultan: College of Engineering, University of Warith Al-anbiyaa, Karbala, Iraq, e-mail: hakimaljobori@gmail.com
Kamaruzzaman Sopian: Solar Energy Research Institute, University Kebangsaan Malaysia, 43600 Bangi, Selangor, Malaysia, e-mail: ksopian@ukm.edu.my

the efficacy of solar heating systems [3]. The effect of nanofluid on a rotating cylinder open to a heat source was investigated. The largest heat transmission occurred at the heat source's corner locations, which was 13.70% more than the heat transfer obtained. Greater cylinder rotating speeds improve heat transfer performance, while increased magnetic strength has the opposite effect. At maximal nanoparticle concentration, the greatest heat transfer augmentation achieved by nanofluids was 94.18% more than water [4]. The effect of nanofluids utilized in photovoltaic/thermal, heat exchangers, and solar collectors was studied. The authors of the previous study [5] created a solar heat pipe storage device for heating applications. For the solar cycle of this system, several nanofluids such as TiO_2, MWCNT, CuO, and H_2O-propylene glycol were utilized. Energy usage declined by 67.7% in August and 42.2% in November [6]. Expanding application renewable energy resources was necessary due to the increased energy demand and the depletion of existing energy sources. The experiment is carried out in broad daylight with a constant flow rate and steady-state conditions. The use of % Al_2O_3 and % crystal nano-cellulose nanofluids increased efficiency of a solar collector by up to 2.48 and 8.46%, respectively, according to the testing data. Furthermore, nanofluids have high to moderate stability. Furthermore, when the temperature increased, the thermal conductivity increased while the viscosity decreased. The heat gain from a solar heating system was increased by using nanofluids [7]. Increased fluid mixing improved the heat uptake and thermal efficiency of a solar thermal system by using twisted ribs and nanofluids. Twisted ribs facilitated heat transmission. The use of nanoparticles increased the heat transfer coefficient by 18% [8]. MWCNT nanofluids were utilized to examine the effectiveness of a solar heating system to deliver hot water and air. The collector efficiency was determined to be related to nanomaterial concentration. The temperature differential for the solar heating system was 14.54°C, with MWCNT nanofluids reaching the greatest temperature of 18.32°C. Reference [9] studied the effect of CuO nanoparticles on solar evacuated pipe heat gain. The thermal efficiency of solar/evacuated tubes was increased by using nanofluids. CuO nanoparticles at 0.03% in the evacuated pipes system offered up to a 14% improvement [10]. The influence of nanofluids on solar thermal systems such as photovoltaic solar thermal, solar heating systems, and geothermal solar thermal systems was investigated [11]. The effect of using different nanofluids on solar wing parabolic surface collectors was explored. In ethylene glycol, Cu nanoparticles and ZrO_2 nanoparticles were combined. The hybrid nanofluid was shown to be the most efficient heat transfer medium. When compared to Cu-EG, ZrO_2-Cu-EG has a lower thermal efficiency of 2.6% and a higher thermal efficiency of 3.6% [12]. The effect of nanofluids on photovoltaic solar efficiency was investigated. The nanofluids improve thermal efficiency by mixing the thermal conductivity of metal nanoparticles with base fluids. It was observed that using 0.2 wt% AL_2O_3, 0.05 wt% Cu, and 1.0 wt% MWCNT, respectively, enhanced efficiency by about 29, 9, and 20–30% [13]. The thermal behavior of a solar-assisted air handling system filled with nanofluid was studied. The results showed that using Al_2O_3 nanoparticles not only increased the loss coefficients but also boosted annual collector effectiveness by 6.1% due to an increase in maximum efficiency. After integrating a nanofluid-based solar system with the air handling unit in July, the energy demand was decreased by 4,700 kW h, resulting in a 17.9% reduction by the heated coil [14]. Nanofluids were used to increase the efficiency of a solar flat plate system. A 25-liter-per-day solar flat plate water heater has been created. Solar flat plate collectors used 0.2–0.4% Al_2O_3 and CuO nanoparticles in distilled water. Nanoparticles increase heat transport in solar flat plate collectors, improving solar water heater efficiency [15]. A breakthrough curtain wall-integrated solar heater needs to be made based on the notion of an energy-harvesting façade that uses solar energy or solar heaters in conjunction with natural circulation loop designs powered by heat transfer processes. This study investigates the thermal performance of a novel curtain wall-integrated solar heater by employing nanofluid as a working fluid, which has superior thermal characteristics to water, to boost the solar heater's heat transfer capabilities. Reference [16] examined the efficiency of a direct absorption solar collector based on nanofluids. When compared to pure water, the presence of nanoparticles boosts incoming radiation absorption. A direct-absorption solar system used nanofluid with an improvement about 10% more efficiency than the efficient solar flat system. A solar collector that uses nanofluids as its working fluid surpasses a flat plate collector in the majority of cases. Reference [17] studied the results of the effect of mixing MWCNT nanofluid with distilled water on the performance of a flat plate solar water collector. Nanofluids' thermophysical properties have been proven to be excellent in solar water collectors. The concentrations of MWCNT particles ranged from 0.10 to 0.30% by volume. The experiments were conducted at a variety of mass flow rates ranging from 1 to 3 LPM. According to the findings, increasing the volume fraction of MWCNT nanofluid from 0.10 to 0.30% boosts collector efficiency by up to 30.5% [18]. The addition of

nanofluids to a solar heating collector improved its performance. Increases in nanofluid volume and flowrates improve collector efficiency. The collector efficiency of nanofluids was 9–17% higher than the base fluid [19]. As working fluids in a rectangular single-phase natural circulation loop, water, Al_2O_3 nanofluid, and TiO_2 nanofluid were tested. When the efficacy factor, temperature differential over heater, and the mass flow rate of NCLs with different working fluids were evaluated, it was shown that increasing particle concentration improves thermal performance, particularly for nanofluids with larger particle sizes [20]. The effect of CeO_2–water nanofluid on the performance of a solar water collector was studied both empirically and theoretically. It performs better due to the improved thermophysical characteristics of the nanofluid, with data revealing that the greatest efficiency of a solar water heater using CeO_2 nanofluid is 78.2%, which is 21.5% higher than when water is used as the base fluid. In experimental research, the greatest collector efficiency of nanofluid was observed at the optimal mass flow rate of 2 LPM [21]. The thermal conductivities of nanofluids and the impact of Cu nanofluids on the efficiency of a solar water heater were examined experimentally. Cu nanofluids at 0.1 wt% and 25 nm boosted the efficiency of a solar water heater by 23.83%. The efficiency of 0.2 wt% Cu nanofluids is lower than that of 0.1 wt% Cu nanofluids. As the nanoparticle size increased, the efficiency of the solar water heater decreased. When compared to the water tank, the peak temperature and highest heat gain of 0.1 wt% nanofluid may be increased by 12.2 and 24.5%, respectively. Reference [22] examined the increase in solar system performance by employing different nanofluids, the efficiency of solar water heaters, photovoltaic thermal systems, thermoelectric solar systems, and geothermal systems. Nanofluids are utilized to improve heat gain for solar heating systems. The effect of cooling using nanofluids on the performance of a CPU system was investigated. Reference [23] examined experientially the influence of solar power on wastewater treatment by using hydrogen as a novel rotated anode reactor with electro-coagulation. Reference [24] studied the effect of water micro-jet impingement to enhance output power and heat gain in the photovoltaic thermal system. References [25,26] investigated the heat transfer enhancement and improvement of the performance for different thermal systems. References [27–34] investigated the effect of jet water for cooling photovoltaic solar system with compound parabolic concentrator. Reference [35] studied the effect of jet water on the bottom for cooling array solar cells on the output power and heat gain. Reference [36] tested experimentally the impact of air jet impingement on the total performance of the air solar system [37]. Nonlinear EHD instability of two superimposed Walters' B fluids moving over porous media was already analyzed in depth. References [38,39] examined the nanofluid flow on a stretched or shrinking surface: insights into partial slips and temperature increases. Reference [40] studied the stability of two Reiner–Rivlin fluids using the He-Laplace technique for nonlinearity. Presented Darcy-Forchheimer Peristaltic Flow Dynamics in Rabinowitsch Fluids: Hall Current and Joule Heating. The development of a nonlinear vibration model for the movement of nanoparticles in the spinning process was done [41]. This study aims to evaluate numerically the influence of different concentrations and nanoparticles diameter of silicon dioxide nanoparticles on improving the heat transfer in solar thermal collector (STC). Water/SiO_2 and pure water are used as circulating fluids with different Reynolds numbers of 5,000–30,000 in the tube with uniform heat flux on the top of the tube of STC.

2 Mathematical model and numerical solution

2.1 Governing equations

Figure 1 displays the design and schematic diagram of STC. Water/SiO_2 and pure water flow with the change in Reynolds numbers from 5,000 to 30,000. The various parameters (type fluid, concentrations of nanoparticles, nanoparticles diameters, and flow rate) were investigated by using CFD in this study. This issue considers a steady, turbulent two-dimensional flow. Newtonian and incompressible fluid (water) is assumed. Given the aforementioned observations, continuity, momentum, energy equations, and turbulence kinetic are the problem's governing equations. A fully developed turbulent flow is applied to the pipe inlet for the STC. The heat flux is applied on top of tube STC. Using an outlet pressure-outlet state, various volume fractions (concentration) of silicon dioxide nanoparticles varied from 0 to 4% with different diameters between dp = 20 nm and dp = 50 nm were examined. The k–ε RNG turbulence model was used in the current study. At the inlet, the turbulence rate was sustained at 1%.

$$\frac{\partial U_i}{\partial X_i} = 0, \tag{1}$$

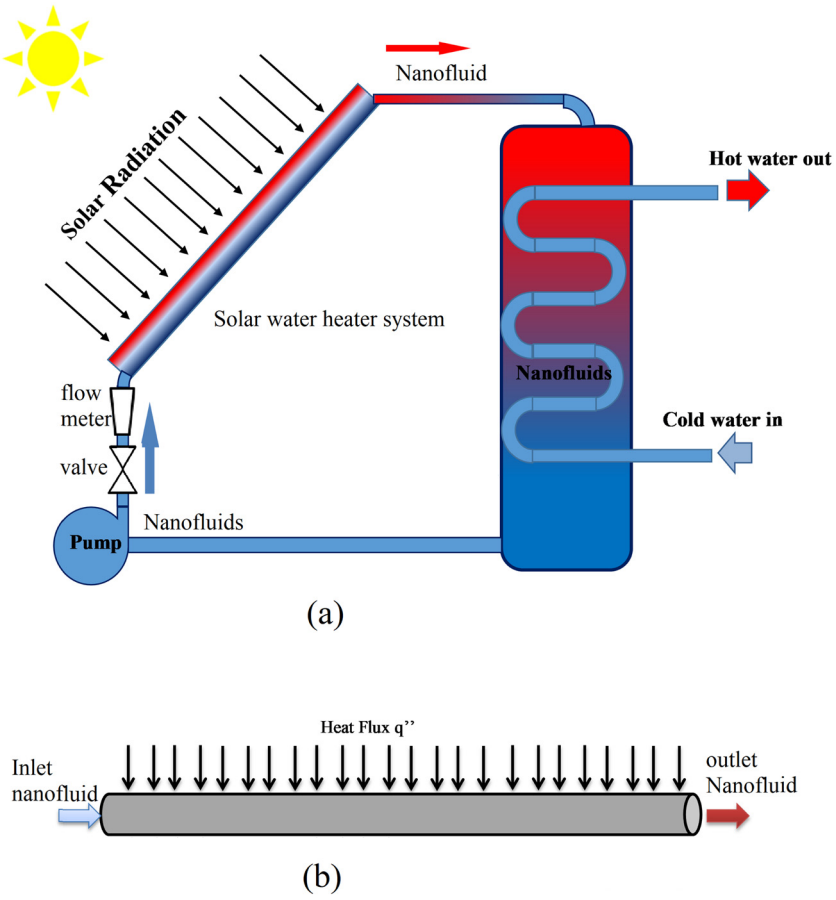

Figure 1: Schematic diagram of (a) the STC and (b) the tube of STC.

$$\rho U_i \frac{\partial U_i}{\partial X_i} = -\frac{\partial P}{\partial X_i} + \frac{\partial}{\partial X_i}\left[\mu\left(\frac{\partial U_i}{\partial X_j} + \frac{\partial U_j}{\partial X_i}\right) - \rho\overline{u_i' u_j'}\right], \quad (2a)$$

$$-\rho\overline{u_i' u_j'} = \mu_t\left(\frac{\partial U_i}{\partial X_j} + \frac{\partial U_j}{\partial X_i}\right) - \frac{2}{3}\delta_{ij}\rho k, \quad (2b)$$

$$\rho C_p U_i \frac{\partial T}{\partial x_i} = \frac{\partial}{\partial x_i}\left[k\frac{\partial T}{\partial x_i} - \rho\overline{u_i' T'}\right], \quad (3)$$

$$\mu_t = \rho C_\mu \frac{K^2}{\varepsilon}. \quad (4)$$

k–ε RNG turbulence method includes the following:

$$\frac{\partial}{\partial x_i}(\rho k u_i) = \frac{\partial}{\partial x_j}\left[\left(\mu + \frac{u_t}{\sigma_k}\right)\frac{\partial k}{\partial x_j}\right] + G_k - \rho\varepsilon, \quad (5)$$

$$\frac{\partial}{\partial x_i}(\rho\varepsilon u_i) = \frac{\partial}{\partial x_j}\left[\left(\mu + \frac{u_t}{\sigma_k}\right)\frac{\partial \varepsilon}{\partial x_j}\right] + C_{1\varepsilon}\frac{\varepsilon}{k}G_k - C_{2\varepsilon}\rho\frac{\varepsilon^2}{k}. \quad (6)$$

G_k is written as follows:

$$G_k = (-\rho\acute{u}_i\acute{u}_j)\frac{\partial u_j}{\partial x_i}. \quad (7)$$

3 Results and discussion

3.1 Effects of nanofluids on heat transfer coefficients

This section evaluates numerically the effect of using water/SiO_2 and pure water as working fluids on heat transfer enhancement for the STC. The relationship between Nusselt numbers and different Reynolds numbers is shown in Figure 2. As demonstrated in the figure, the Nusselt numbers of STC using water/SiO_2 are higher than the base fluid (water) for all Reynolds numbers because of the high thermal conductivity of the nanofluid. The improvement in heat transfer is also associated with the collision between silicon dioxide nanoparticles and the tube wall, resulting in enhanced energy exchange rates. Nusselt numbers increase with the increasing Reynolds number. Among test fluids, the higher heat transfer enhancement by the flow of water/SiO_2 than pure water. The Nu_{avg} enhances 25% by using water/SiO_2 nanofluid as the working fluid at Re = 5,000 and 15% at Re = 30,000.

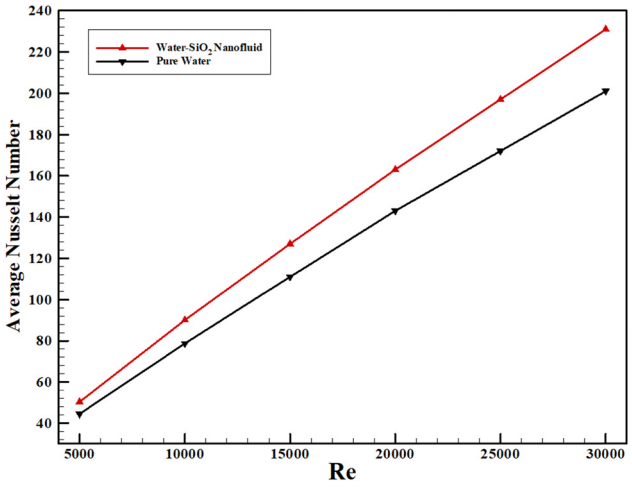

Figure 2: Reynolds number and Nusselt number variation using water/SiO_2 nanofluid and pure water for STC.

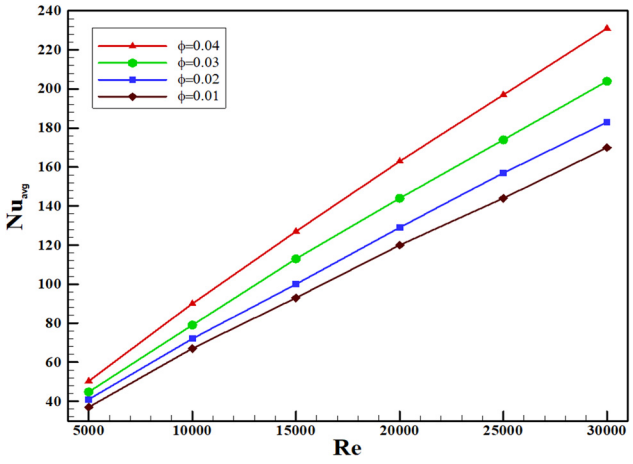

Figure 4: The average Nusselt number versus Reynolds number for various volume fractions, ϕ of water/SiO_2 with dp = 20 nm.

Figure 3 presents the variation in Reynolds number with Skin friction coefficients by using water/SiO_2 nanofluid and pure water for STC. It is noted that the skin friction factor decreases with increases in the Reynolds number for both fluids. Water/SiO_2 nanofluid has a higher skin friction factor than pure water.

3.2 Effects of various volume fractions for silicon dioxide nanoparticles

This section presents the impact of concentrations of silicon dioxide nanoparticles on the friction factor and heat transfer enhancement in STC. Figure 4 illustrates how various concentrations (ϕ = 1–4%) of SiO_2 nanoparticles affect the Nusselt number and skin friction coefficients. In this study, Reynolds numbers vary from 5,000 to 30,000. When the Reynolds number increases, the average Nusselt number also increases. It is found that all Reynolds numbers using volume fractions of 4% of water/SiO_2 provide the highest Nusselt number due to the high thermal conductivity of SiO_2 nanoparticles. The Nu_{avg} improves 31% at the lowest Reynolds number by using water/SiO_2 nanofluid to reduce the number of SiO_2 nanoparticles from (ϕ = 1%) to (ϕ = 4%) and 42% at the highest Reynolds number of 30,000. Figure 5 presents the result of the skin friction coefficient versus the Reynolds number for various concentrations of SiO_2 nanoparticles with dp = 20 nm. The skin friction coefficient increases with increasing the concentration of the nanofluid. Increasing nanofluid

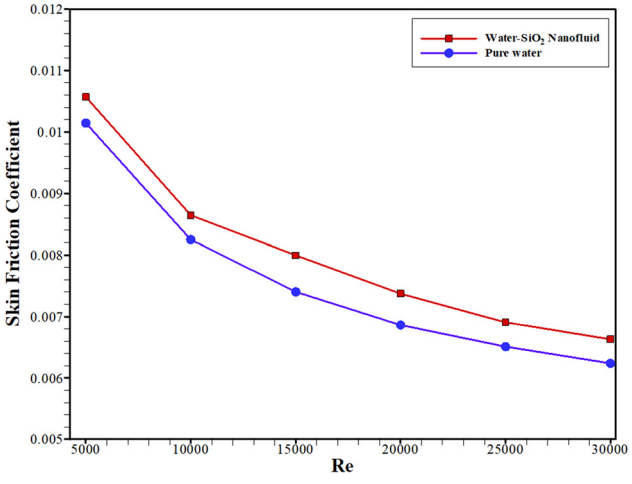

Figure 3: Reynolds number and skin friction coefficient variation using water/SiO_2 nanofluid and pure water for STC.

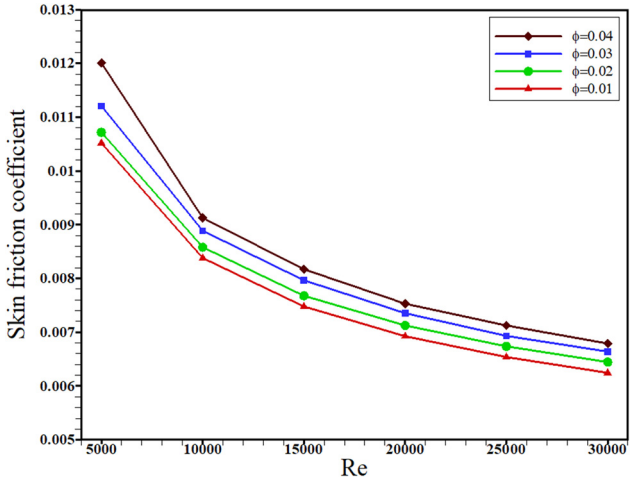

Figure 5: The skin friction coefficient, Reynolds number variation for various volume fractions of metal oxide nanoparticles, and ϕ of water/SiO_2 nanofluid with dp = 20 nm.

concentration typically results in the increased fluid viscosity, which limits the fluid movement. Figure 6 presents the results of the Nusselt number enhancement ratio versus the Reynolds number for various volume fractions of metal oxide nanoparticles, ϕ of water/SiO_2 nanofluid with dp = 20 nm. The highest concentration of SiO_2 nanoparticles (ϕ = 4%) provides the highest ratio of enhancement for the Nusselt number in STC.

3.3 Effects of the diameter for silicon dioxide nanoparticles

The impact of the size of silicon dioxide nanoparticles on heat transfer enhancement and friction factor is presented in this study. Diameters of different SiO_2 nanoparticles (dp = 20–50 nm) were tested with fix concentration of 4%. As shown in Figure 7, the decrease in the nanoparticle diameter led to an increase in the Nusselt number across all Reynolds numbers. The lowest size of SiO_2 nanoparticles (dp = 20 nm) provides the highest Nusselt number. The active dynamic viscosity of nanofluid increases with the decreasing nanoparticle diameter resulting in enhanced heat transfer. The Nu_{avg} improves 35% by using water/SiO_2 nanofluid at lowest size SiO_2 nanoparticles (dp = 20 nm) at Re = 5,000 and 15% at Re = 30,000 in STC. Figure 8 illustrates the Reynolds numbers versus skin friction coefficients for various metal oxide nanoparticles diameters of water/SiO_2 nanofluid with ϕ = 4%. It is found that the skin friction coefficients decrease as diameters of SiO_2 nanoparticles decrease. Figure 9 presents the results of the Nusselt number enhancement ratio versus Reynolds number for various sizes of SiO_2 nanoparticles (ϕ = 4%). The lowest size SiO_2 nanoparticles (dp = 20 nm) provides the highest ratio of enhancement for Nusselt number in STC.

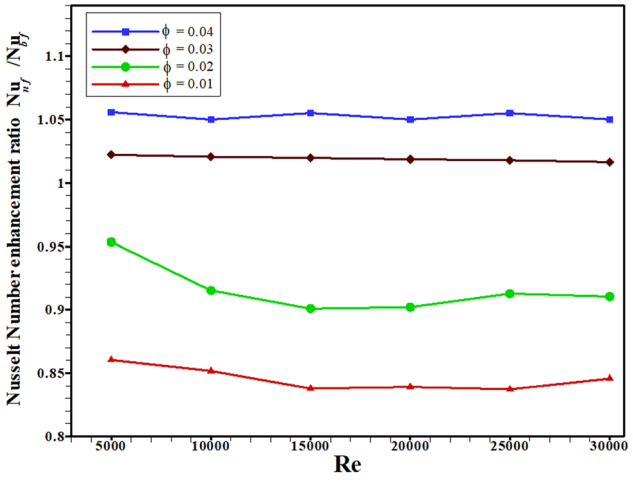

Figure 6: The enhancement ratio, Reynolds number variation for various volume fractions of metal oxide nanoparticles, and ϕ of water/SiO_2 nanofluid with dp = 20 nm.

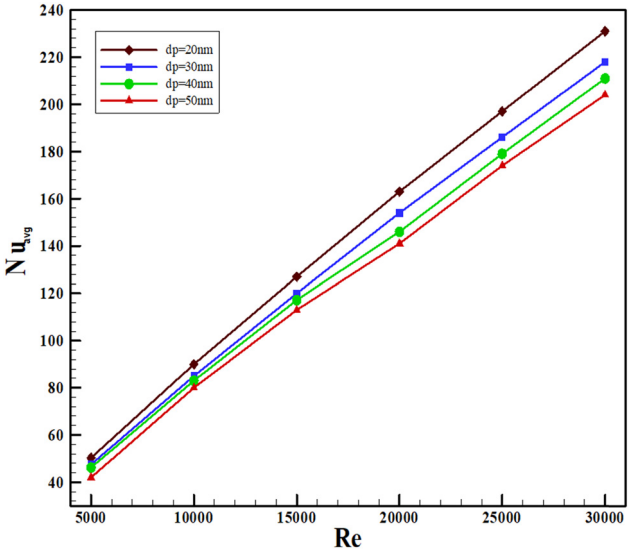

Figure 7: Average Nusselt number and Reynolds number variation for various diameters of SiO_2 nanoparticles of water/SiO_2 nanofluid with ϕ = 0.04.

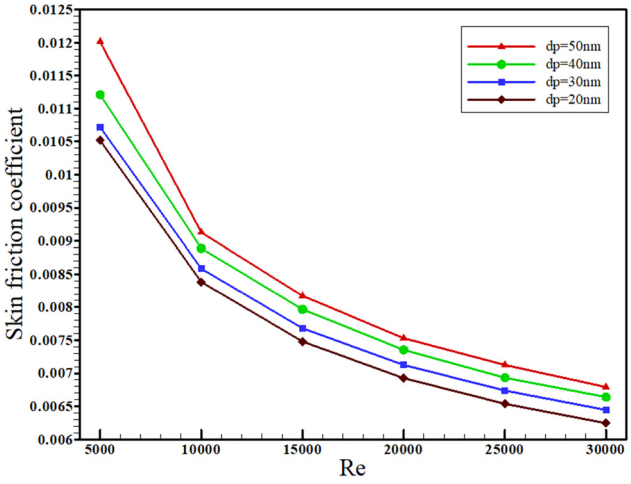

Figure 8: Reynolds numbers and skin friction coefficient variation for various diameters of SiO_2 nanoparticles of water/SiO_2 nanofluid with ϕ = 4%.

4 Conclusions

The current numerical study discusses the impact of size and concentrations of silicon dioxide nanoparticles on

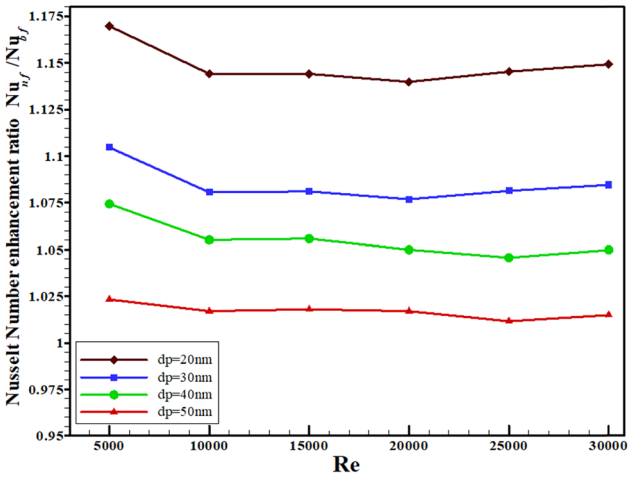

Figure 9: The enhancement ratio versus Reynolds number for various metal oxide nanoparticles diameters of water/SiO_2 nanofluid with ϕ = 0.04.

heat transfer enhancement ratio and friction factor for STC. The computational simulation illustrates the influence of the flow of water/SiO_2 and pure water inside the pipe on the enhancement of the performance of the STC. Different concentrations of SiO_2 nanoparticles are used (ϕ = 1–4%) with several nanoparticle diameters (dp = 20–50 nm). The water/SiO_2 and pure water flow under different Reynolds numbers 5,000–30,000. The following points are important to highlight:

- The average Nusselt numbers Nu_{avg} improved by increasing Reynolds numbers for both fluids.
- The Nu_{avg} increases with the increased of the concentration of SiO_2 nanoparticles.
- The water/SiO_2 with nanoparticles concentration of ϕ = 5% and nanoparticle diameter of dp = 20 nm has the highest Nusselt number.
- The Nu_{avg} enhances 25% by using water/SiO_2 nanofluid as the working fluid at Re = 5,000 and 15% at Re = 30,000.
- The skin friction factor decreases with increase in the Reynolds number for both fluids. Water/SiO_2 nanofluid has a higher skin friction factor than pure water.
- The Nu_{avg} improves 31% at Re = 5,000 using the high concentration of SiO_2 nanoparticles of ϕ = 4 and 42% at Re = 30,000.
- The decrease in the nanoparticle diameter led to an increase in the Nusselt number across all Reynolds numbers.
- The lowest size of SiO_2 nanoparticles (dp = 20 nm) provides the highest Nusselt number.

Nomenclature

A	cross section area
C_p	specific heat (J kg^{-1} K^{-1})
d	diameter of pipe
f	friction factor
k	thermal conductivity (W m^{-1} K^{-1})
k_B	Boltzmann constant (=1.3807 × 10^{-23} $J^{-1}K^{-1}$)
l	turbulence length scale
Nu	average Nusselt number
P	pressure (Pa)
PP	pumping power
Pr	Prandtl number
q	uniform heat flux (W m^{-2})
Re	Reynolds number
T	temperature (K)

Greek letters

α	cross section area
α	thermal diffusivity
δ	distance between particles (m)
ε	dissipation rate of turbulent kinetic energy
	nanoparticles volume fraction
μ	dynamic viscosity (N s m^{-2})
μ	tturbulent or eddy viscosity
ν	kinematics viscosity (m^{-2} s^{-1})
ρ	density (kg m^{-3})

Conflict of interest: Authors state no conflict of interest.

References

[1] Akbarzadeh M, Rashidi S, Karimi N, Ellahi R. Convection of heat and thermodynamic irreversibilities in two-phase, turbulent nanofluid flows in solar heaters by corrugated absorber plates. Adv Powder Technol. 2018;29(9):2243–54. doi: 10.1016/j.apt.2018.06.009.

[2] Akram N, Montazer E, Kazi SN, Soudagar ME, Ahmed W, Zubir MN, et al. Experimental investigations of the performance of a flat-plate solar collector using carbon and metal oxides based nanofluids. Energy. 2021;227:120452. doi: 10.1016/j.energy.2021.120452.

[3] Ali MM, Akhter R, Alim MA. Hydromagnetic mixed convection in a triangular shed filled by nanofluid and equipped with rectangular heater and rotating cylinders. Int J Thermofluids. 2021;11:100105. doi: 10.1016/j.ijft.2021.100105.

[4] Bretado-de los Rios MS, Rivera-Solorio CI, Nigam KDP. An overview of sustainability of heat exchangers and solar thermal applications with nanofluids: A review. Renew Sustain Energy Rev. 2021;142:110855. doi: 10.1016/j.rser.2021.110855.

[5] Daghigh R, Zandi P. An air and water heating system based on solar gas combined with nanofluids and phase change materials. J Clean Prod. 2021;311:127751. doi: 10.1016/j.jclepro.2021.127751.
[6] Farhana K, Kadirgama K, Mohammed HA, Ramasamy D, Samykano M, Saidur R. Analysis of efficiency enhancement of flat plate solar collector using crystal nano-cellulose (CNC) nanofluids. Sustain Energy Technol Assess. 2021;45:101049. doi: 10.1016/j.seta.2021.101049.
[7] Fattahi A. On the rotary concentrated solar collector containing twisted ribs and MgO-Ag-water nanofluid. J Taiwan Inst Chem Eng. 2021;124:29–40. doi: 10.1016/j.jtice.2021.05.013.
[8] Ganesh Kumar P, Balaji K, Sakthivadivel D, Vigneswaran VS, Velraj R, Kim SC. Enhancement of heat transfer in a combined solar air heating and water heater system. Energy. 2021;221:119805. doi: 10.1016/j.energy.2021.119805.
[9] Ghaderian J, Sidik NA, Kasaeian A, Ghaderian S, Okhovat A, Pakzadeh A, et al. Performance of copper oxide/distilled water nanofluid in evacuated tube solar collector (ETSC) water heater with internal coil under thermosyphon system circulations. Appl Therm Eng. 2017;121:520–36. doi: 10.1016/j.applthermaleng.2017.04.117.
[10] Said Z, Hachicha AA, Aberoumand S, Yousef BAA, Sayed ET, Bellos E. Recent advances on nanofluids for low to medium temperature solar collectors: energy, exergy, economic analysis and environmental impact. Prog Energy Combust Sci. 2021;84:100898. doi: 10.1016/j.pecs.2020.100898.
[11] Salilih EM, Abu-Hamdeh NH, Alsulami RA, Rawa MJ, Aljinaidi AA, Alazwari MA, et al. Annual performance analysis of small scale industrial waste heat assisted solar tower power plant and application of nanofluid. J Taiwan Inst Chem Eng. 2021;124:216–27. doi: 10.1016/j.jtice.2021.04.019.
[12] Sheikholeslami M, Farshad SA, Ebrahimpour Z, Said Z. Recent progress on flat plate solar collectors and photovoltaic systems in the presence of nanofluid: A review. J Clean Prod. 2021;293:126119. doi: 10.1016/j.jclepro.2021.126119.
[13] Khdair AI, Rumman GA, Basha M. Integrating a nanofluid-based solar system with air handling unit to reduce energy usage: Case studies in Saudi Arabia. J Taiwan Inst Chem Eng. 2021;128:338–45. doi: 10.1016/j.jtice.2021.06.011.
[14] Munuswamy DB, Madhavan VR, Mohan M. Comparison of the effects of Al_2O_3 and CuO nanoparticles on the performance of a solar flat-plate collector. J Non-Equilibr Thermodyn. 2015;40(4):265–73. doi: 10.1515/jnet-2015-0019.
[15] Kulkarni PP, Joshi MP. Study of thermal performance of an innovative curtain-wall-integrated solar heater with nanofluid. Int J Mech Prod Eng Res Dev. 2020;10(3):47–60. doi: 10.24247/ijmperdjun20205.
[16] Tyagi H, Phelan P, Prasher R. Predicted efficiency of a Low-temperature Nanofluid-based direct absorption solar collector. J Sol Energy Eng Trans ASME. 2009;131(4):0410041–7. doi: 10.1115/1.3197562.
[17] Rajput NS, Shukla DDB, Sharma SK, Rajput D. Thermal analysis of MWCNT/distilled water nanofluid on the efficiency of flat plate solar collector. Int J Mech Eng Technol. 2017;8:233–40.
[18] Karami M, Akhavan-Bahabadi MA, Delfani S, Raisee M. Experimental investigation of CuO nanofluid-based Direct Absorption Solar Collector for residential applications. Renew Sustain Energy Rev. 2015;52:793–801. doi: 10.1016/j.rser.2015.07.131.
[19] Ghorbanali Z, Talebi S. Investigation of a nanofluid-based natural circulation loop. Prog Nucl Energy. 2020;129:103494. doi: 10.1016/j.pnucene.2020.103494.
[20] Stalin PMJ, Arjunan TV, Matheswaran MM, Sadanandam N. Experimental and theoretical investigation on the effects of lower concentration CeO_2/water nanofluid in flat-plate solar collector. J Therm Anal Calorim. 2019;135(1):29–44. doi: 10.1007/s10973-017-6865-4.
[21] He Q, Zeng S, Wang S. Experimental investigation on the efficiency of flat-plate solar collectors with nanofluids. Appl Therm Eng. 2014;88:165–71. doi: 10.1016/j.applthermaleng.2014.09.053.
[22] Elsheikh AH, Sharshir SW, Mostafa ME, Essa FA, Ali MKA. Applications of nanofluids in solar energy: A review of recent advances. Renew Sustain Energy Rev. 2018;82:401–12. doi: 10.1016/j.rser.2017.10.108.
[23] Hasan HA, Alquziweeni Z, Sopian K. Heat transfer enhancement using nanofluids for cooling a Central Processing Unit (CPU) system. J Adv Res Fluid Mech Therm Sci. 2018;51(2):145–57.
[24] Naje AS, Chelliapan S, Zakaria Z, Ajeel MA, Sopian K, Hasan HA. Electrocoagulation by solar energy feed for textile wastewater treatment including mechanism and hydrogen production using a novel reactor design with a rotating anode. RSC Adv. 2016;6(12):10192–204. doi: 10.1039/c5ra26032a.
[25] Hasan HA, Sopian K, Ameen KA. Numerical investigation of Microjet impingement of water for cooling photovoltaic solar cell. J Adv Res Fluid Mech Therm Sci. 2018;51(1):71–9.
[26] Dezfouli MM, Sopian K, Al-Shamani AN, Hasan HA, Abed AM, Elbreki AM, et al. Energy saving potential of solar cooling systems in hot and humid region. ARPN J Eng Appl Sci. 2017;12(18):5241–4.
[27] Hasan HA, Sopian K, Jaaz AH, Al-Shamani AN. Experimental investigation of jet array nanofluids impingement in photovoltaic/thermal collector. Sol Energy. 2017;144:321–34. doi: 10.1016/j.solener.2017.01.036.
[28] Al-Waeli AHA, Sopian K, Chaichan MT, Kazem HA, Hasan HA, Al-Shamani AN. An experimental investigation of SiC nanofluid as a base-fluid for a photovoltaic thermal PV/T system. Energy Convers Manag. 2017;142:547–58. doi: 10.1016/j.enconman.2017.03.076.
[29] Al-Shamani AN, Sopian K, Mat S, Hasan HA, Abed AM, Ruslan MH. Experimental studies of rectangular tube absorber photovoltaic thermal collector with various types of nanofluids under the tropical climate conditions. Energy Convers Manag. 2016;124:528–42. doi: 10.1016/j.enconman.2016.07.052.
[30] Sopian K, Alwaeli AHA, Hasan HA, Al-Shamani AN. Advances in high efficiency photovoltaic thermal solar collectors. J Adv Res Fluid Mech Therm Sci. 2018;47(1):1–7.
[31] Rukman NS, Fudholi A, Utari PA, Aisyah CN, Purwanto AJ, Pramana RI, et al. Bi-fluid cooling effect on electrical characteristics of flexible photovoltaic panel. J Mechatron Electr Power Veh Technol. Jul. 2021;12(1):51–6. doi: 10.14203/j.mev.2021.v12.51-56.
[32] Hameed Jaaz A, Hasan HA, Sopian K, Kadhum AAH, Gaaz TS, Al-Amiery AA. Outdoor Performance analysis of a photovoltaic thermal (PVT) collector with Jet impingement and compound parabolic concentrator (CPC). Mater (Basel). 2017;10(8):888. doi: 10.3390/ma10080888.

[33] Ameen KA, Al-Dulaimi MJ, Abrahem HA, Hasan HA. Experimental study to increase the strength of the adhesive bond by increasing the surface area arrangement. IOP Conf Ser Mater Sci Eng. 2020;765:1–10.
[34] Ameen KA, Abdulrasool Hasan H, Al-Dulaimi MJ, Abed AM, Al-Qrimli HF. Improving the performance of air conditioning unit by using a hybrid technique. MethodsX. Jan. 2022;9:101620. doi: 10.1016/J.MEX.2022.101620.
[35] Jaaz AH, Hasan HA, Sopian K, Bin Haji Ruslan MH, Zaidi SH. Design and development of compound parabolic concentrating for photovoltaic solar collector: Review. Renew Sustain Energy Rev. 2017;76:1108–21. doi: 10.1016/j.rser.2017.03.127.
[36] Hasan HA, Sopian K, Fudholi A. Photovoltaic thermal solar water collector designed with a jet collision system. Energy. 2018;161:412–24. doi: 10.1016/j.energy.2018.07.141.
[37] Aboghrara AM, Baharudin BTHT, Alghoul MA, Adam NM, Hairuddin AA, Hasan HA. Performance analysis of solar air heater with jet impingement on corrugated absorber plate. Case Stud Therm Eng. 2017;10:111–20. doi: 10.1016/j.csite.2017.04.002.
[38] He J-H, Moatimid GM, Sayed A. Nonlinear EHD instability of two-superposed Walters' B fluids moving through porous media. Axioms. 2021;10(4):258. doi: 10.3390/axioms10040258.
[39] He JH, Abd Elazem NY. Insights into partial slips and temperature jumps of a nanofluid flow over a stretched or shrinking surface. Energies. 2021;14(20):6691. doi: 10.3390/en14206691.
[40] He J-H, Moatimid GM, Mostapha DR. Nonlinear instabilityof two streaming-superposed magnetic Reiner-Rivlin FluidsbyHe-Laplace method. J Electroanal Chem. 2021;895:115388. doi: 10.1016/j.jelechem.2021.115388.
[41] Yao X, He JH. On fabrication of nanoscale non-smooth fibers with high geometric potential and nanoparticle's non-linear vibration. Therm Sci. 2020;24(4):2491–7.